Techno-economic evaluation on a hybrid technology for low hydrogen concentration separation and purification from natural gas grid

Maria Nordio [a], Solomon Assefa Wassie [a], Martin Van Sint Annaland [c], D. Alfredo Pacheco Tanaka [b], José Luis Viviente Sole [b], Fausto Gallucci [a,]*

[a] *Inorganic Membranes and Membrane Reactors, Sustainable Process Engineering, Department of Chemical Engineering and Chemistry, Eindhoven University of Technology, De Rondom 70, 5612 AP, Eindhoven, the Netherlands*

[b] *Tecnalia, Energy and Environment Division, Mikeletegi Pasealekua 2, 20009 San Sebastian-Donostia, Spain*

[c] *Chemical Process Intensification, Department of Chemical Engineering and Chemistry, Eindhoven University of Technology, De Rondom 70, 5612 AP, Eindhoven, the Netherlands*

HIGHLIGHTS

- Different configurations were proposed to reach a high hydrogen recovery and purity.
- It is possible to maximize either the recovery or the purity at similar costs.
- Both metallic supports and ceramic supports were considered for Pd membranes.
- Systems with more membrane stages result in lower costs at higher purities.

ARTICLE INFO

ABSTRACT

Hydrogen can be stored and distributed by injecting into existing natural grids, then, at the user site separated and used in different applications. The conventional technology for hydrogen separation is pressure swing adsorption (PSA). The recent NREL study showed the extraction cost for separating hydrogen from a 10% H_2 stream with a recovery of 80% is around 3.3—8.3 US$/kg. In this document, new system configurations for low hydrogen concentration separation from the natural gas grid by combining novel membrane-based hybrid technologies will be described in detail. The focus of the manuscript will be on the description of different configurations for the direct hydrogen separation, which comprises a membrane module, a vacuum pump and an electrochemical hydrogen compressor. These technological combinations bring substantial synergy effect of one-another while improving the total hydrogen recovery, purity and total cost of hydrogen. Simulation has been carried out for 17 different configurations; according to the results, a configuration of two-stage membrane modules (in series) with a vacuum pump and an electrochemical hydrogen compressor (EHC) shows highest hydrogen purity (99.9997%) for 25 kg/day of hydrogen production for low-pressure grid. However, this configuration shows a higher electric consumption (configuration B) due to the additional mechanical compressor between the two-stage membrane modules and the EHC. Whereas, when the compressor is excluded, and a double skin Pd membrane (PdDS) module is used in a single-stage while connected to a vacuum pump (configuration A5), the hydrogen purity (99.92%)

slightly decreases yet the power consumption considerably improves (1.53 times lower). Besides to these two complementary configurations, the combination of a single membrane module, a vacuum pump and the electrochemical compressor has been also carried out (configuration A) and results show that relatively higher purity can be achieved. Based on four master configurations, this document presents a different novel hybrid system by integrating two to three technologies for hydrogen purification combined in a way that enhances the strengths of each of them.

Introduction

The consensus in hydrogen production from renewable energy sources (during off-peak hours), to be injected into existing natural gas grids for initial (or long-term) storage and subsequent use in a range of different applications (power generation, heat provision, transport applications such as gas-fuelled urban buses or passenger cars), has raised [1,2]. The maximum hydrogen blend level is 5–20%, potentially even 25% depending on the gas grid infrastructure. Injecting the green hydrogen into the gas grid offers several advantages, such as sector coupling, gas decarbonization, energy storage and easy distribution (with the existing infrastructure). The maximum blend level of hydrogen into the gas grid varies greatly across European countries; for instance, in Belgium and UK up to 3% (and the last projects aim at 20%) while in Netherlands and Germany up to 10–14% (in volume percent). However, the main question here is how efficiently and at what cost can the injected hydrogen be separated and purified from the natural gas grid. Taking the Netherlands as a reference case, we proposed a novel system configuration for a 10% H_2 mixture separation with higher hydrogen recovery factor, higher purity and lower energy consumption compared to the existing commercially available technology.

The conventional technology for hydrogen separation is pressure swing adsorption (PSA) [3,4]. This system is based on sorbent material which is used to adsorb the non-hydrogen component at elevated pressure. In such a system, the separated and purified hydrogen is delivered at high pressure while the non-hydrogen compound is discharged at lower pressure. However, if the incoming gas mixture is from a high-pressure stream (natural gas grid), the non-hydrogen stream (NG) needs to be compressed to be sent back to the natural gas grid. For that, two mechanical compressors are required in the system. The first compressor is to reach the adsorption pressure for separation of hydrogen while the second one is necessary for compressing the natural gas back to the grid. However, if we employ such a system for the separation of hydrogen in relatively low concentrations from a hydrogen-methane mixture, this system would require a substantial amount of compression energy and compressor capital for the reinjection of depleted hydrogen back to the grid. This makes PSA technology quite uneconomical.

The PSA system works efficiently at large scale and higher hydrogen concentrations, but if the hydrogen in the stream is lower than 10%, the gas needs to be pressurized to a high pressure ratio, which makes the PSA option inefficient [4]. The PSA unit is sized as a function of the amount of impurities in the gas mixture that needs to be purified. With low hydrogen concentrations, the PSA units become very large. Besides, the higher the adsorption pressure, the purer the hydrogen discharged, but the larger the energy consumption required to pressurize back to the grid (the non-hydrogen compound). The recent NREL study showed the extraction cost for separating hydrogen from a 10% H_2 stream with a recovery of 80% is up to 8.3 US$/kg for a recovery rate in the range between 100 and 1000 kg/day [5]. This report assesses only the separation costs, while other costs such as injection and hydrogen losses along the pipeline are not considered. The calculated energy consumption for separation of 10% H_2 concentration is 20 kWh/kg_{H2}. The lower the hydrogen rate separated, the higher the extraction costs expected. The hybrid technology considered in this manuscript is for hydrogen separation of 25 kg/day, hence a hydrogen separation cost higher than 8.3 US$/kg will be considered when working with a PSA unit.

PSA units are commercially available in the market for large scale systems, while for small scale units, the hydrogen separation costs of such a system substantially increases. In general, some of the main limitations of the PSA unit for small scale hydrogen separation and purification from natural gas are [6,7]:

- It is very energy intensive
- It is very expensive
- Needs an additional component, such as a compressor to recompress the natural gas to the original natural gas grid pressure (capital cost).
- Needs several separation columns to purify the low hydrogen concentration (at least five)
- The efficiency is very low for small scale applications

Therefore, we are proposing an alternative technology that offers better efficiency, lower costs, superior separation ability for low concentration, easy scalability and simplicity. The proposed configuration is described below along with the main advantages of the configuration.

The work aims to propose different configurations for low hydrogen concentration separation from the natural gas grid, which combine two or more of these components: Pd–Ag membrane, CMSM (carbon molecular sieve membrane), EHC

(electrochemical hydrogen compressor), vacuum pump and TSA. The integration of TSA has been done only when sweep gas is applied on the membrane permeate side. The TSA aims is to further purify the hydrogen stream, removing the water remaining in the permeate stream. The proposed configurations have been analysed to study the hydrogen purity and energy consumption. Finally, an economic evaluation was carried out considering OPEX (operating expense) and CAPEX (capital expense) costs. A sensitivity analysis was done based on membrane type and support, permeate pressure, membrane and EHC lifetime and sweep gas flow rate to optimize the separation system.

The model described in previous work [8–11], which predicts the Pd–Ag membrane performance accounting for the concentration polarization and mass transfer limitations has been integrated in the Aspen simulation for a proper description of the membrane unit of the hybrid technology. The experimental results based on hydrogen permeance and purity obtained on CMSM [12–15], have been adopted to simulate the CMSM unit of the proposed technology. The EHC model, proposed in previous studies [8,16], was integrated in the simulation for the description of the compressor component in each configuration.

Proposed configurations for hydrogen separation

Alternative novel hybrid configurations based on well-known units (membrane, electrochemical hydrogen compressor, vacuum pump and temperature swing adsorption unit) are proposed for low hydrogen content separation from a natural gas mixture. These technological combinations bring substantial synergy effects, while improving the total hydrogen recovery, purity and reduce the total cost of hydrogen. The main advantages of this novel concept are: high hydrogen recovery, high purity, high efficiency, less energy consumption, lower costs and easy scalability.

Two different membrane types have been considered for the proposed configurations: ceramic supported Pd–Ag and alumina composite carbon molecular sieve (Al-CMS) membranes. The membrane unit is responsible for the first main purification, especially in the case where two membrane modules are used. The choice of the membrane type to be used in a membrane module must consider both performance and costs. Pd–Ag membranes are highly selective to hydrogen and allow the production of a pure hydrogen stream. However, these membranes suffer from H_2 embrittlement at low temperatures and high pressure as well as surface contamination by sulphur-containing species, requiring cleaning steps of the feed gas and high temperature during separation. Furthermore, Pd is an expensive noble metal, which encourages the search for cheaper solutions. Carbon molecular sieve membranes are becoming an alternative to the high costs of Pd–Ag membranes due to their much lower costs and the fact that they can operate at low temperatures, where Pd–Ag membranes suffer from instabilities or low permeabilities. CMSM, composed of microporous, amorphous high-carbon materials, have emerged as promising materials for the gas

separation applications because of their characteristics, such as superior thermal resistance, chemical stability in corrosive environments, lower cost and proven stability at high feed pressures (up to 69 bar) [17–20]. Through adsorption and molecular sieving mechanisms, the CMSMs are particularly useful in gas separation, and separation can be achieved even between gases with almost similar molecular size. MXene molecular sieve membranes and MOF membranes, which were considered in the proposed manuscript, are promising technology thanks to the separator factor in the presence of mixtures, which is exceeding the Robeson upper bound [21,22].

The electrochemical hydrogen compressor on the other hand, is the component responsible to further purify and separate the hydrogen left in the outlet retentate side of the membrane [23,24].

Unlike TSA, the PSA cannot avoid the need to pressurize the hydrogen and the off-gas (1 or 2 compressors). With the TSA technology [25] used in the European project HyGrid, the use of a temperature change rather than a pressure change to drive the desorption leads to lower operational costs for heat compared to electric power. Moreover, with TSA each vessel needs 1–1.5 cycles/day, whereas with PSA 700–800 cycles/day are required.

Different configurations for the integration of these components have been studied for an efficient hydrogen separation in terms of purity and costs. The effect of sweep gas and vacuum (to decrease the partial pressure on the permeate side of membranes) have also been studied and assessed, to further confirm the results obtained in Nordio et al. [8]. Single and multiple membrane modules have been integrated into the hybrid system, to compare the cost and purity of separation. Configurations based on Pd–Ag and CMS membranes were compared as separation technology to purify hydrogen. Membrane parameters such as the hydrogen permeance and selectivity were changed to study their influence on the hydrogen recovery, purity and costs.

Four different master configurations (A-D as reported in Table 1) have been selected as base cases to describe the integration of the different components, while a sensitivity analysis on the retentate pressure, the amount of sweep gas, the membrane type, a single or multistage system, the quantity of hydrogen separated by EHC and the total flow rate have been performed to analyse the optimal configuration in terms of purity and economics.

In Table 1, the term c-PdDS is used to describe a ceramic supported double-skin Pd–Ag membrane, m-Pd is a metallic supported Pd–Ag membrane and c-Pd is a ceramic supported Pd–Ag (4–5 μm) membrane, c-tPd is a thin Pd–Ag (2–3 μm) ceramic supported membrane while CMSM is a composite alumina carbon molecular sieve membrane (Al-CMSM). Configurations with two membrane modules in series have been considered, therefore Membrane 2 in Table 1 indicates the second module. The data used for the membranes are taken from experimental results from literature or obtained in dedicated experiments not reported in this paper [8,12,23]. For all configurations, removing of sulphur compounds from NG, and remixing of those in the NG before reinjection are not

Table 1 – Description of details of the different configurations; c-PdDS: ceramic supported double-skin Pd—Ag membrane, m-Pd: metallic supported Pd—Ag membrane; CMSM composite alumina-carbon molecular sieve membrane, c-Pd; ceramic supported Pd—Ag membrane (4–5 μm); c-tPd: ceramic supported thin Pd—Ag membrane (2–3 μm).

Configuration	Membrane type	Membrane permeance [mol/s/m²/Pa]	Membrane ideal-selectivity	Membrane 2 permeance	Membrane 2 ideal selectivity	Retentate pressure [bar]	Permeate pressure [bar]	Sweep gas flow rate [mol/h]
A	c-PdDS	$2 \cdot 10^{-6}$	65,000	–	–	8	0.15	–
A1	m-Pd	10^{-6}	200,000	–	–	8	0.15	–
A2	c-PdDS	$2 \cdot 10^{-6}$	65,000	–	–	8	0.15	–
A3	c-PdDS	10^{-6}	200,000	–	–	40	0.15	–
A4	CMSM	$2 \cdot 10^{-6}$	65,000	–	–	40	0.15	–
A5	c-PdDS	$2 \cdot 10^{-6}$	65,000	–	–	8	0.15	–
A6	EHC	–	–	–	–	8	8	–
B	c-tPd	$4 \cdot 10^{-6}$	5000	$2 \cdot 10^{-6}$	20,000	8	0.15	–
C	c-tPd	$4 \cdot 10^{-6}$	5000	$2 \cdot 10^{-6}$	20,000	40	3	–
C1	CMSM	$5 \cdot 10^{-8}$	1000	$2 \cdot 10^{-6}$	20,000	40	3	–
C2	c-tPd	$4 \cdot 10^{-6}$	5000	$2 \cdot 10^{-6}$	20,000	40	2.5	–
C3	c-tPd	$4 \cdot 10^{-6}$	5000	$2 \cdot 10^{-6}$	20,000	40	2	–
C4	CMSM	$7 \cdot 10^{-8}$	550	$2 \cdot 10^{-6}$	20,000	40	2.5	–
C5	CMSM	$7 \cdot 10^{-8}$	550	$2 \cdot 10^{-6}$	20,000	40	2	–
D	c-tPd	$4 \cdot 10^{-6}$	5000	$2 \cdot 10^{-6}$	20,000	8	1	1000
D1	c-PdDS	$2 \cdot 10^{-6}$	65,000	–	–	8	1	1000
D2	m-Pd	10^{-6}	200,000	–	–	8	1	1000

considered. The humidity removal before reinjection has been considered.

Configuration A

Fig. 1 shows the process flow diagram of master configuration named A; with this configuration, the incoming stream, at 8 bar (low-pressure industrial NG grid), is initially pre-heated in a heat exchanger to the working temperature of 400 °C using the outlet retentate stream. At the same time this stream is being cooled down, and then the heater supplies the additional heat needed to reach the membrane working temperature. After the heater, the stream is sent to the membrane module. It is a double-skin Pd—Ag ceramic supported membrane with a hydrogen permeance of $2 \cdot 10^{-6}$ mol/s/m²/Pa and a H_2/CH_4 selectivity at 1 bar of 65,000. The retentate side of the membrane is at the same pressure as the stream coming from the grid. The permeate side was kept at 100 mbar by using a vacuum pump (to increase the driving force via the membrane). The permeate stream is cooled down with a cooler before entering the vacuum pump. The retentate side of the membrane is then sent to an electrochemical

hydrogen compressor (EHC) with a protonic membrane resistance of 6 mΩ and 350 cells in parallel with a working temperature of 65 °C for further hydrogen separation and purification. The retentate outlet stream is cooled down in the heat exchanger previously mentioned while heating the stream coming from the grid. Indeed, the EHC gives better performances at higher temperatures but the proper water management for the humidification of the protonic membrane must be considered when choosing the operating conditions. Besides, the hydrogen coming from the outlet cathode side is kept at the same pressure as the grid. The purified hydrogen from the permeate side of the membrane and the cathode side of the electrochemical hydrogen compressor are then mixed after depressurization of the stream from the EHC. The outlet anode side of the electrochemical hydrogen compressor is sent back to the grid with no or low hydrogen concentration in the stream (depends on which configuration is chosen).

Configuration A has been studied changing different parameters to understand their influence on the system performance. Indeed, the hydrogen recovered by the EHC has been decreased to 23.13%, in configuration A2, while in configuration A1, the membrane support was changed considering a metallic supported Pd—Ag membrane. The retentate pressure was increased up to 40 bar (medium pressure industrial NG grid) (A3) and a CMSM and a retentate pressure of 40 bar was adopted for configuration A4. For heating the inlet stream, electricity has been considered. It should be noted that the results of analysis for higher pressure NG grids (80 bar and higher) are not reported in this manuscript, but the conclusions in relative terms are similar. Configuration named A5 is presented in the Appendix. It is based only on the membrane module and the vacuum pump while the EHC is not included. A6 is the configuration which includes only the EHC and is described in detail in the Appendix.
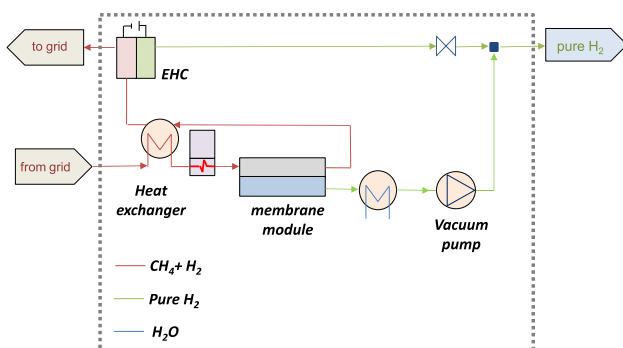

to grid
EHC
from grid
Heat exchanger
membrane module
Vacuum pump
pure H₂

— $CH_4 + H_2$
— Pure H_2
— H_2O

Fig. 1 – Process flow diagram of configuration A.

Configuration B

In this configuration, as depicted in Fig. 2, two membrane modules with a mechanical compressor in between, a vacuum pump and an EHC have been combined. The first membrane module is an ultra-thin Pd–Ag ceramic supported membrane with a hydrogen permeance of $4 \cdot 10^{-6}$ mol/s/m^2/Pa and H$_2$/CH$_4$ selectivity of 5000. The difference is in the membrane layer thickness, indeed in this case the thickness is between 2 and 3 μm. The working pressure is 8 bar in the retentate and 100 mbar in the permeate, and the temperature is 400 °C. The second membrane module is a Pd–Ag ceramic supported membrane with a hydrogen permeance of $2 \cdot 10^{-6}$ mol/s/m^2/Pa and H$_2$/CH$_4$ selectivity of 20,000. The retentate pressure of the second membrane module is 8 bar, which is obtained through the mechanical compressor. The permeate pressure of the second membrane is atmospheric. The first membrane is responsible for an initial purification while the second membrane is in charge of increasing the hydrogen purity. The stream which comes from the grid has the same feed rate and composition as of the other master configuration and is also initially electrically heated in a heat exchanger and heater. The outlet retentate stream of the first membrane module is cooled to the working temperature of the EHC.

The outlet anode side of this EHC is sent back to the natural gas grid. The permeate side of the first module is kept at vacuum conditions. The second membrane is at atmospheric conditions. The outlet stream of the vacuum pump is then compressed and sent to the second membrane module after the two cascaded heat exchangers. The retentate stream from the second membrane module (mainly some impurities and remaining inextricable H$_2$) is sent back to the first module for further purification. The purified hydrogen from the second membrane module and the cathode side of the EHC is then mixed and sent to the end-users.

Configuration C

Configuration C is depicted in Fig. 3. It includes two membrane modules in series, an electrochemical hydrogen compressor and a vacuum pump. The stream coming from the grid is preheated in a heat exchanger and a heater before being fed to the membrane module. The first membrane module is a carbon molecular sieve membrane that works at the operating temperature of 70 °C, while the second membrane is a Pd–Ag ceramic supported membrane that operates at 400 °C. The outlet retentate side of the first module is sent to the electrochemical hydrogen compressor. The permeate side is fed to the second membrane module. It is worth noting that the retentate side of the second membrane module works at a lower pressure than the first membrane, indeed no mechanical compressor is required in between. The permeate side of the second membrane is at vacuum conditions.

The retentate pressure of the first membrane is at the same pressure as the grid which in this specific case is 40 bar, while the permeate pressure has been kept at 3 bar. The proposed configuration is used for recovering hydrogen coming from a medium-pressure natural gas grid. The retentate side of the first membrane module is sent to the EHC, which works at 65 °C. The hydrogen recovered from the second membrane and the electrochemical hydrogen compressor is collected and sent to the final users. A variant of this master configuration is C1, where the first membrane module is a ceramic supported Pd–Ag membrane. A second variation consists of a different permeate pressure, which are configurations C2 and C3, where the permeate pressure is respectively 2.5 and 2 bar and the same membrane type as configuration C1 is adopted. In configuration C4 and C5, where CMSMs are used, the permeate pressure is reduced to 2.5 and 2 bar.

Configuration D

The proposed master configuration D, as depicted in Fig. 4, is based on two membrane modules in series (with sweep gas in the first module), a mechanical compressor, an electrochemical hydrogen compressor and a TSA unit.

The inlet stream has been heated up electrically while the steam has been produced with heaters and a boiler. Configuration D1 and D2 based only on one membrane module with sweep gas have been described in the Appendix.
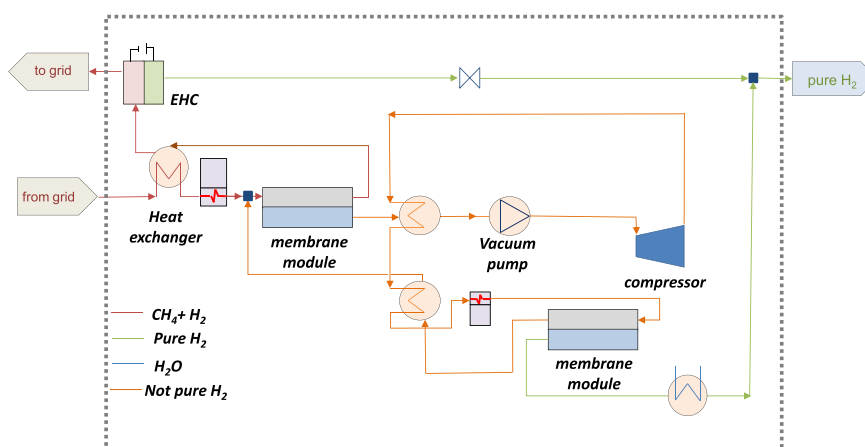

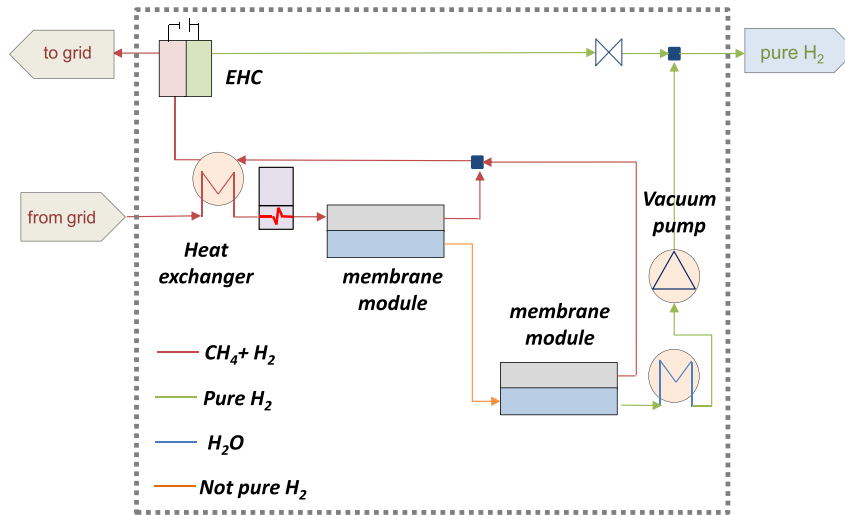**Fig. 2** – **Process flow diagram of configuration B.**

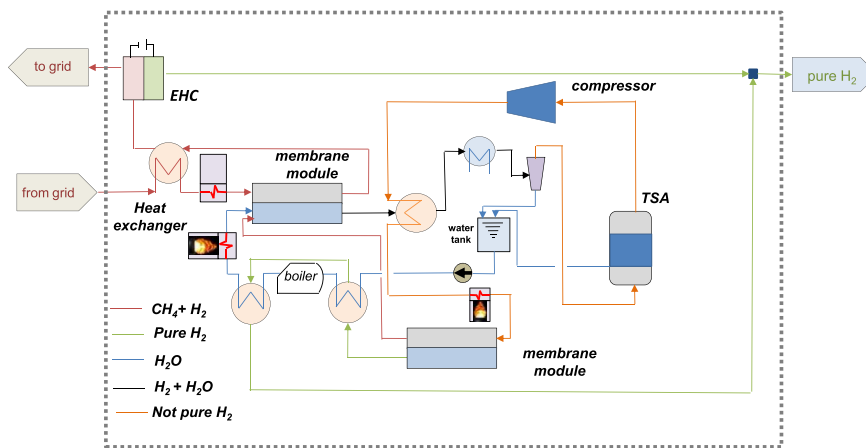**Fig. 3 – Process flow diagram of configuration C.**

Fig. 4 – Process flow diagram of configuration D.

Economic evaluation

An economic evaluation is needed to verify the economic advantage in terms of final hydrogen separation cost of each of the proposed configurations, comparing to commercially available PSA technology. The hydrogen separation cost has been analysed also to evaluate different parameters to optimize the performance of the hybrid systems, such as membrane type, membrane support, retentate pressure, permeate pressure and heating system through electricity or natural gas.

Capital and variable costs have been evaluated to calculate the final hydrogen separation cost. Investment costs are equal to the product between the total overnight cost (TOC) and capital charge factor (CCF). The TOC is the bare erected cost (BEC) plus the contingency, container, transportation and assembly costs. The final separation cost is the sum of the investment, O&M which includes labour cost, insurance and maintenance and variable costs [26].

The hydrogen separation cost has been calculated as the ratio between the sum of the capital (CAPEX) and operational costs (OPEX) and the hydrogen flow rate separated as reported in Eq. (1).

$$\text{cost of hydrogen separation} = \frac{\text{CAPEX} + \text{OPEX}_{\text{variable}} + \text{O\&M}_{\text{fixed}}}{\dot{m}_{H_2}}$$

(1)

The costs of all the units considered in the hybrid system, which will be used later to calculate the bare erected costs, have been estimated based on the scale-up factor correlation, shown in Eq. (2)

$$C = nC_0 \left(\frac{S}{nS_0} \right)^f$$

(2)

where C_0 is the cost of the component based on literature data, S_0 is the capacity of the scaling parameter, which is also based on literature data, S is the capacity that has to be scaled, n is the number of units to be considered and the f is the scaling

factor. The prices and scaling parameters of all the units used in this work are taken from the Price Booklet of the Dutch Association of Cost Engineers (DACE) [30–32]. The equations used for the CAPEX calculations are summarized in Table 2. Differently, the operational expenses (OPEX) can be differentiated between the fixed costs, which mostly refer to labour costs, maintenance and insurance, and the variable costs which include electricity, heat consumption and sorbent replacement.

In Fig. 5, the production cost for the different membrane modules is proposed divided in support, membrane layer and production costs. It is worth noting that the metallic supported membranes show the highest membrane cost due to the support, which is more expensive. Carbon molecular sieve membranes are the cheapest thanks to the lower costs of membrane layer and production in comparison to Pd–Ag membranes. Besides, the following two assumptions have been made:

- Europe has been the selected scenario for all the different calculations
- The hybrid technologies have been considered to separate 25 kg/day of hydrogen

Results

Comparison of required membrane area, energy consumption and hydrogen purity

Between the different proposed configurations, it is possible to reach the highest purity (99.99%) when (Fig. 1) working with two membrane modules in series thanks to the further purification. This is obtained from two membrane stages combined with the EHC. The results are described in Table 3. Besides, with this configuration, the quality of natural gas for the end-users is improved, as it lets a very low hydrogen concentration back into the natural gas grid. On the other

hand, the energy consumption required for this configuration is slightly higher, in particular for configuration D2, where sweep gas is applied. The more energy efficient configuration, based on two membrane modules, considers CMSM in the first module, because of the lower operating temperature associated to CMSM in comparison to the Pd–Ag membrane. Moreover, Configuration B has an additional mechanical compressor, which increases the required energy consumption.

Configuration A1 shows an extremely high purity thanks to the metallic Pd–Ag membranes, which exhibit an extremely high selectivity at the expense of increased cost. The drawback of using metallic supported Pd–Ag membranes is the large surface area required due to low hydrogen permeance. Indeed, configuration A1, requires 2.92 m^2 compared to 1.62 m^2 for configuration A, where a double-skin membrane is adopted (the membrane type is the only difference between the two configurations). Configuration A and A2 have the same layout with the difference in the lower hydrogen recovery from the EHC in A2. Since only 23.13% of the final hydrogen is separated by the EHC in configuration A2, the membrane surface area of configuration A2 is higher. A trade-off between membrane area and energy consumption is visible here and this will be studied in detail in the techno-economic evaluation. It causes an increase in the membrane area, which will negatively affect the final hydrogen separation cost, on the other hand, it reduces the electricity consumption due to the lower hydrogen rate separated by the electrochemical hydrogen compressor. From the results it is possible to notice that by increasing the retentate pressure, as in configuration A3 (where the retentate pressure is 40 bar), the purity drops from 99.93% to 99.42% due to a more pronounced permeation of the contaminant gas. However, configuration A3 requires a lower membrane area (1.07 m^2) thanks to the higher applied pressure. A4 and A3 have the same pressure; the only difference is the type of membrane used. Indeed, A4 has a CMSM, while A3 is Pd–Ag membrane. From the results shown in Table 3, the configuration with CMSM requires a higher surface area to separate the same

| Table 2 – Economic evaluation assumptions [27–29].	
Capital costs (CAPEX)	
Plant component	Cost
Component A	A
Component B	B
Component C	C
Component D	D
BEC (Bare erected costs)	A+B+C+D
Container cost	12,000 €
Transportation cost	4000 €
Assembly cost	5000 €
Contingency cost	15% BEC
CCF (Capital charge factor)	0.04
TOC (Total overnight cost)	BEC + Container + transportation + assembly + contingency cost
Investment	TOC·CCF
Operating cost (OPEX)	
Labor cost	0.3% TOC
Maintenance cost	2% TOC
Insurance	3% TOC
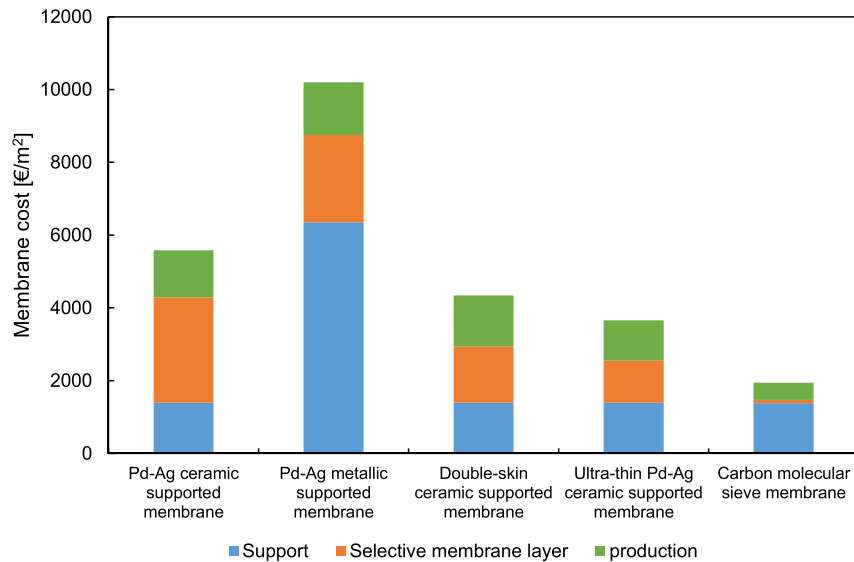
Fig. 5 – Membrane production cost for the different membranes type considered including support, selective membrane layer and production costs [32].

hydrogen flow rate and the purity drops since the CMSM is less selective than Pd–Ag membranes, but an economic evaluation is needed to compare the costs when using Pd–Ag membranes or CMSM. Moreover, the electricity consumption is reduced in configuration A4 because the membrane operates at 70 °C, instead of 400 °C, which reduces dramatically the electricity consumption needed. The hydrogen permeance associated with the CMSM is one order of magnitude lower than the Pd–Ag membrane, thus the membrane surface area required is increased to 5.27 m² in configuration A4. It is worth noting, that the membrane cost for CMSM is cheaper than the Pd–Ag membrane, thanks to the reduced material costs and reduced production costs as fewer steps are involved as shown in Fig. 5.

Configuration D2 is based on a membrane module where sweep gas is used to increase the driving force, and this configuration requires more membrane area compared to the configuration in which vacuum is applied at the permeate side. Indeed, the membrane surface area is 2.53 m², in contrast to 1.62 m² for configuration A (with the same layout but applying vacuum instead), due to the more pronounced mass transfer limitations in the presence of sweep gas. Indeed, there is a pressure drop due to the sweep gas, which reduces the actual driving force over the membrane compared to the case where vacuum is applied [8,9,33–35] and this phenomenon was accounted for in the model.

The hydrogen purity is slightly lower than in configuration A, as mass transfer limitations reduce the hydrogen concentration, thereby increasing the contaminant concentration. The electricity consumption increases dramatically for the configuration where sweep gas is adopted, associated with the fact that the heat exchangers, which in configuration An allow

Table 3 – Description of hydrogen separation flux, purity, electricity and heat consumption for the overall configurations.								
Configuration	Membrane area 1 [m²]	Membrane area 2 [m²]	Hydrogen separated [kg/day]	Purity from membrane [%]	% H$_2$ from EHC	Total purity [%]	Electricity consumption [kWh/kg$_{H2}$]	Heat consumption [kWh/kg$_{H2}$]
A	1.62	–	25	99.92	34.92	99.93	5.19	–
A1	2.92	–	25	99.9876	34.92	99.99	5.05	–
A2	2.8	–	25	99.92	23.13	99.94	4.29	–
A3	1.07	–	25	99.41	34.92	99.42	5.09	–
A4	5.27	–	25	99	34.92	99	4.36	–
A5	3.85	–	25	99.92	0	99.92	3.94	–
A6	–	–	25	–	100	100	12.64	–
B	2.42	0.5	25	98.75	34.92	99.9997	7.95	–
C	6.32	0.5	25	91.61	34.92	99.99	5.62	–
C1	2.97	0.5	25	96.28	34.92	99.99	6.38	–
C2	2.51	0.62	25	96.11	34.92	99.99	6.30	–
C3	2.23	0.78	25	96.02	34.92	99.99	6.22	–
C4	5.85	0.62	25	91.53	34.92	99.99	5.48	–
C5	5.33	0.78	25	91.4	34.92	99.99	5.40	–
D	3.67	0.5	25	99.94	32.92	99.95	8.02	11.23
D1	2.53	–	25	99.9	34.92	99.91	6.23	11.23
D2	4.22	–	25	99.96	34.92	99.97	6.29	11.23

the inlet stream to reach the working temperature, in configuration D2 are mainly responsible for steam production. Indeed, heaters are needed because it is not possible to recover the heat from the outlet retentate stream to heat the inlet retentate stream. The heat consumption includes only the energy required to boil the steam.

In configuration A5, the electrochemical hydrogen compressor is not included in the system (while the rest of the layout is identical to A) because, as it will be detailed later, the capital cost of the EHC contributes quite significantly to the final separation cost. For this reason, the proposed configuration adopts only the membrane module and a vacuum pump. Obviously, the membrane area increases (3.85 m^2), while the electricity consumption drops because there is no consumption associated with the EHC. It is worth noting that the membrane area required in configuration A5 is close to the membrane area of the sweep gas case, in which a fraction of the separated hydrogen flow is due to the EHC. It is a further proof of the extremely intensive mass transfer limitations when applying sweep gas in comparison to applying vacuum.

As mentioned previously, configuration B which includes two membrane modules and the EHC, is one of the most efficient configurations in terms of hydrogen purity. On the other hand, the electricity consumption is increased due to the mechanical compressor required to reach the retentate inlet pressure of the second membrane stage. Note the higher membrane area required for the first membrane module compared to configuration A due to the necessity to have similar HRF (hydrogen recovery factor) (compared to the other configurations) to allow a hydrogen separation of 25 kg/day. The membrane surface area for this configuration is 2.42 m^2.

Configuration D is based on two membrane modules in series with a mechanical compressor in between, an electrochemical hydrogen compressor and sweep gas is applied to the permeate side of the membrane. A higher purity is reached although energy and heat consumption are quite significant. The required membrane surface area (3.67 m^2) is extremely high due to the concentration polarization, as explained previously.

Configurations C and C1 are proposed as interesting configurations to reduce the electricity consumption, keeping two membrane modules in series. Indeed, in these configurations the first membrane and the stream coming from the grid is at 40 bar and the permeate stream of the first membrane module works at 3 bar, while the second membrane module, when vacuum is applied, has already a relevant pressure difference to be able to further separate and recover the hydrogen. Configuration C has an ultra-thin Pd–Ag membrane in the first module and a Pd–Ag ceramic supported membrane in the second one; while C1 differs from the CMSM in the first module.

The electricity consumption drops in comparison to configuration B, at the expense of increased membrane surface area due to the lower driving force in the first membrane module. In configuration C1 a membrane surface area of 2.97 m^2 is needed. An economic evaluation is required to compare the hydrogen separation cost associated with the different proposed configurations.

In configuration C1, the first membrane module is a ceramic Pd–Ag membrane whereas in configuration C2 and

C3 the permeate pressure of the first membrane module (which is the retentate pressure of the second module), is respectively at 2.5 and 2 bar. As mentioned previously, the membrane area for configuration C is very high due to the low hydrogen permeance of CMSM and the relatively low driving force since 3 bar at the permeate is applied. For this reason, the membrane surface area is 6.32 m^2 in configuration C. Configurations C4 and C5 are based on C2 and C3 layout but using CMSM instead of Pd–Ag membranes. The proposed configurations consider 40 bar as retentate pressure, which is the high-level grid pressure, but are not applicable for low-pressure level grid due to the extremely low driving force if 8 bar is considered. A slight reduction in the final separation cost can be observed for configurations C2 and C3 compared to C1 and in configurations C4 and C5 compared to C thanks to the reduction in electricity consumption associated with the lower pressure at which the mechanical compressor works.

Configuration A6 consists only of the EHC for a comprehensive comparison and techno-economic evaluation, and the hydrogen separation is achieved only through the electrochemical hydrogen compressor. An HRF of 83.25% was achieved with an energy consumption of 12.63 kWh/kg$_{H2}$. The final purity achieved is 100% thanks to the polymeric membrane which allows only hydrogen protons to pass through. If the separation is based only on the electrochemical hydrogen compressor, the energy consumption is extremely high, even if the applied voltage for the separation is 0.3 V.

Economic comparison for 8 bar NG grid pressure

To perform a techno-economic evaluation, the method proposed in Economic evaluation has been considered. The final hydrogen separation and the capital cost for the different configurations to separate hydrogen from a natural gas grid which has a pressure of 8 bar are depicted in Fig. 6 and Fig. 7.

In Fig. 6, where the capital cost distribution is shown, it is possible to notice that the main component affecting the CAPEX is the electrochemical hydrogen compressor, except for configurations A1, D2 and C. In these three configurations (respectively the single stage Pd–Ag membrane, the single stage with sweep gas and the double membrane modules without mechanical compressor and higher permeate pressure) the membrane module has a higher impact. These mentioned configurations are either with a metallic supported membrane or without the EHC. The metallic support has higher costs and the hydrogen permeance is reduced which increases the surface area to separate the same amount of hydrogen.

According to the results, the best configurations from a hydrogen separation cost point of view, are configurations A5 and A, which are respectively the system without the electrochemical hydrogen compressor (only membrane module and vacuum) and the configuration with membrane, EHC and vacuum (in which 34.92% of hydrogen is recovered via the EHC).

Comparing these configurations, the case without electrochemical hydrogen compressor (configuration A5) has a lower energy consumption (3.94 kWh/kg$_{H2}$) and a lower hydrogen purity (99.92%) The configuration A shows a slightly higher purity (99.94%) at the expense of an increased
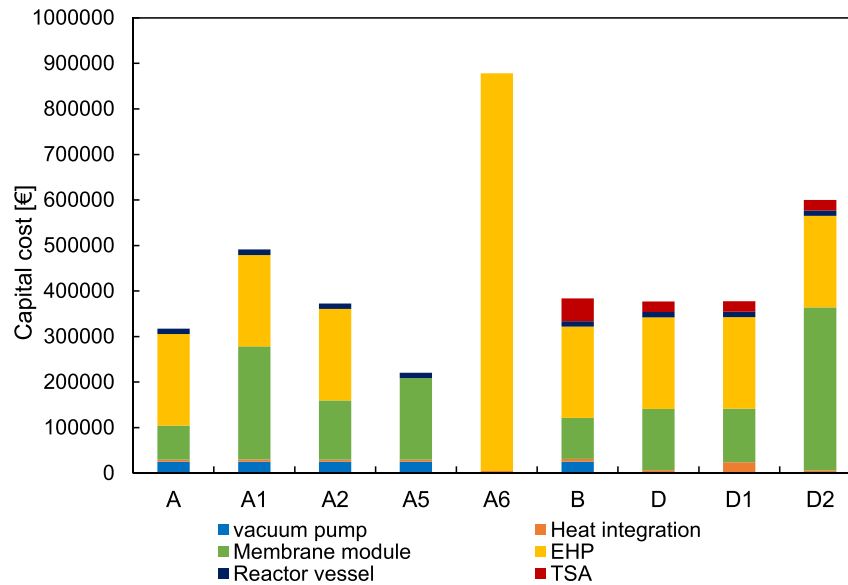
Fig. 6 – Capital cost distribution for the different configurations to separate H_2 from low-pressure natural gas grid.
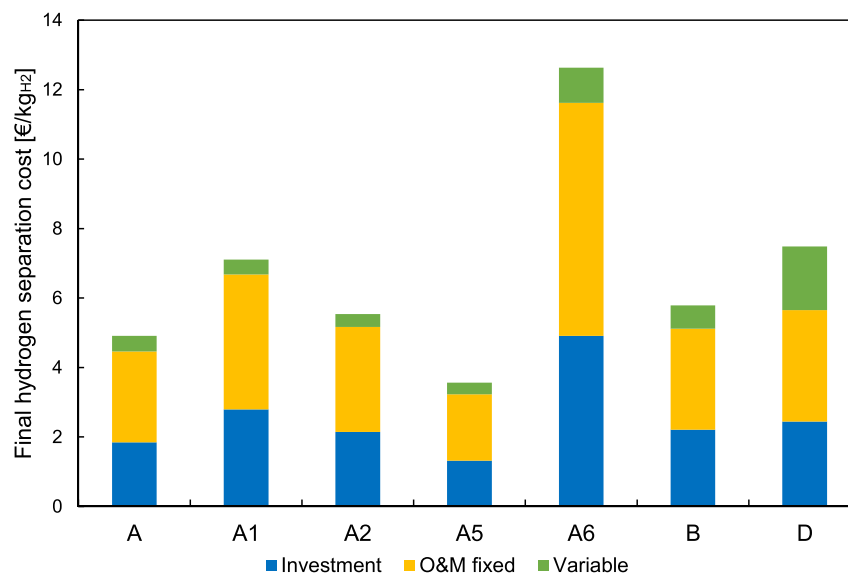

Fig. 7 – Final hydrogen separation cost distribution for the different configurations to separate H_2 from low-pressure natural gas grid.

energy consumption (5.19 kWh/kg_{H2}). A trade-off between these two systems in terms of energy consumption and hydrogen purity is visible. A techno-economic analysis is required to evaluate the economic advantages of one configuration over the other.

It is worth noting that configuration A5 shows the cheapest hydrogen separation cost for all the considered configurations (3.56 €/kg_{H2}), indeed it has only 0.02% purity less than configuration A, while the hydrogen separation cost is 25.05% less than configuration A. In all the considered configurations, the O&M fixed costs have more impact on the final separation cost than the investment and variable cost. Configuration D2 which reaches a hydrogen purity of 99.97%, has the highest hydrogen separation cost of all the considered configurations,

except for configuration A6 which uses only the electrochemical hydrogen compressor.

To optimize the separation, it is important to focus on the hydrogen purity, energy consumption and hydrogen separation cost. Between the configurations which separate hydrogen from a natural gas grid at 8 bar, the ones that reach above 99.99% hydrogen purity are cases B and A6 (respectively the configuration with two membrane modules and the mechanical compressor in between and the configuration with only the EHC). For configuration A6 the energy consumption and the final hydrogen separation cost are extremely high: 12.64 kWh/kg_{H2} and 12.63 €/kg_{H2}. The optimal configuration to work at 8 bar (low grid pressure) is configuration B. Two membrane stages give an added value to the separation thanks to the combination of high purity (99.99%) and low

separation cost (5.78 €/kg$_{H2}$). The drawback of configuration B is the high energy consumption of 7.95 kWh/kg$_{H2}$.

Depending on the final users, configuration A5 (based on a membrane module and a vacuum pump) could be considered interesting since it has a lower separation cost (3.56 €/kg$_{H2}$) than configuration B, but also a lower purity (99.92%). Configurations A and A5 are very similar, indeed they differ only for the EHC, which is included in configuration A. Although they present comparable hydrogen purity, the relevant energy consumption and capital cost of the EHC, demonstrate configuration A5 is more convenient from the cost and consumption approach.

As mentioned previously, configuration A6 has the highest energy consumption, because only the EHC is used to separate 25 kg/day of hydrogen, moreover according to the economic evaluation, it is also the more expensive configurations (12.63 €/kg$_{H2}$). A combination of membrane modules, EHC and vacuum pump is more convenient to decrease the energy consumption and final separation cost.

Economic comparison for 40 bar NG grid pressure

In Fig. 8 and Fig. 9, the results of capital costs and final hydrogen separation cost are depicted for the configurations which separate hydrogen from the natural gas grid at 40 bar.

The electrochemical hydrogen compressor has the highest impact on the investment costs. Configurations A3 and A4 (based on a membrane module, a vacuum pump and the EHC), which reach a purity of 99.41 and 99.00%, respectively, show average separation cost: 4.55 and 4.44 €/kg$_{H2}$, for the purification level obtained. The energy consumptions are respectively 5.09 and 4.36 kWh/kg$_{H2}$. Configuration A4 is based on carbon molecular sieve membranes, while configuration A3 uses ceramic supported Pd/Ag membranes; hence it is important to note that from an energy consumption and economic point of view, configuration A4 is more beneficial, where CMSMs are adopted. On the other hand, configurations C4 and C5 (configurations at 40 bar with two membrane

modules without mechanical compressor in between and respectively with Pd—Ag and CMS membrane in the first module) have a final hydrogen separation cost of 5.30 and 4.81 €/kg$_{H2}$, which is only slightly higher than configurations A3 and A4 (configurations at 40 bar with one membrane module, respectively Pd—Ag and CMS membrane) but guaranteeing a hydrogen purity of 99.99%. The negative drawback is the slightly higher electric consumption (5.38 and 5.30 kWh/kg$_{H2}$) compared to low-level pressure configurations, especially in comparison to configuration A5 (basic system without the EHC).

Configurations C4 and C5 show a better performance in terms of energy consumption and final separation cost compared to configurations C2 and C3, where the only difference is the membrane type adopted (respectively Pd—Ag for C4 and C5 and CMSM for C2 and C3). As mentioned previously, CMSMs are more convenient than Pd—Ag ceramic supported membranes.

Sensitivity analysis

After the description of the different proposed configurations, a sensitivity analysis based on membrane and EHC lifetime, the amount of hydrogen separated by the EHC, the permeate pressure and sweep gas flow rate has been performed to elucidate the influence of each of these parameters on hydrogen separation costs.

The first parameter to be analysed is the membrane and EHC lifetime. Indeed, in the previous description, the membrane lifetime has been considered to be 3 years for the Pd—Ag membranes [36], 5 years for the CMSM and 7 years for the EHC [37—40]. Considering the research studies on these technologies, the membrane lifetime is likely to improve in the following decades, a techno-economic analysis has been performed changing the membrane lifetime from 3 to 25 years. Increasing the membrane lifetime, according to Fig. 10, has a significant impact on the final hydrogen separation cost, and the same effect is observed when the EHC lifetime is
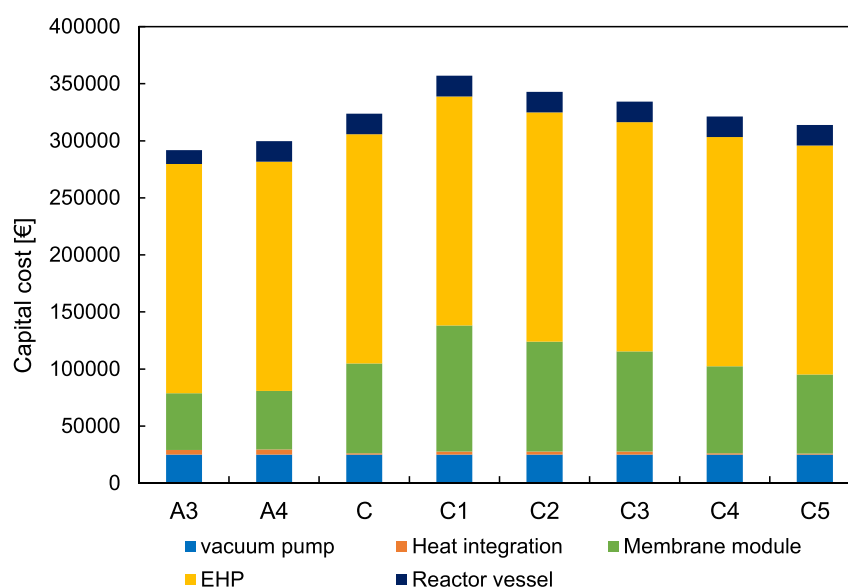

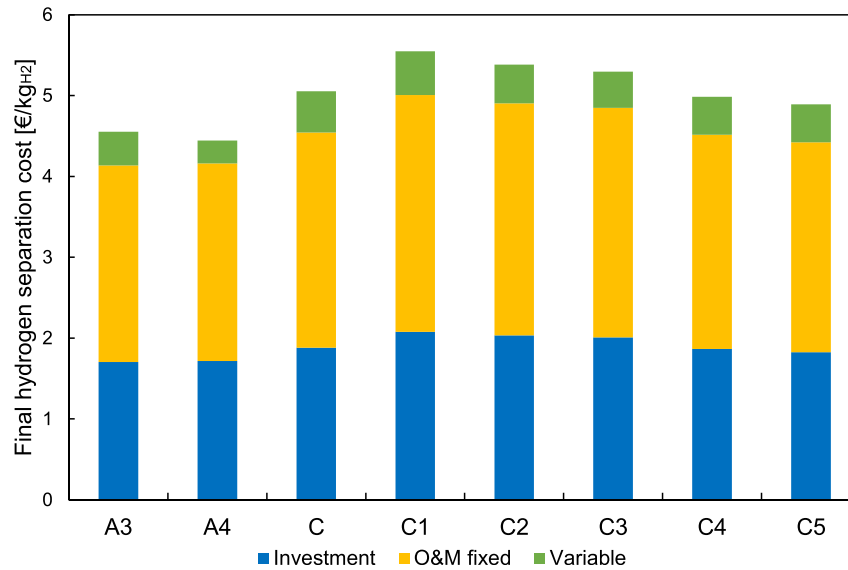**Fig. 8** — **Capital cost distribution for the different configurations to separate H$_2$ from high-pressure natural gas grid.**

Fig. 9 − **Final hydrogen separation cost distribution for the different configurations to separate H$_2$ from high-pressure natural gas grid.**
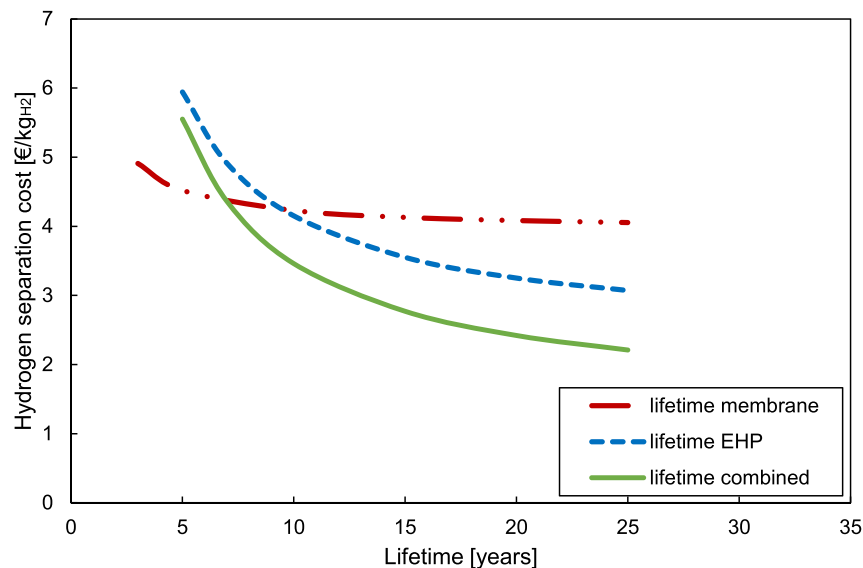

Fig. 10 − **Membrane and EHC lifetime impact on hydrogen separation cost for configuration A.**

increased. The optimal conditions are found when both the membrane and EHC lifetime is increased. Indeed, a reduction in the final hydrogen separation cost from 5.94 to 2.21 €/kg$_{H2}$ could be obtained.

Configurations A and A2 have as the only substantial difference the relative amount of hydrogen recovered from the EHC (34.92 and 23.13% respectively). The final separation cost is reduced when a higher recovery is achieved with the EHC, because it reduces the membrane surface area needed for the separation. On the other hand, the energy consumption is increased because the EHC is responsible for a higher recovery. In Fig. 11, the results for the hydrogen separation cost and energy consumption as a function of the hydrogen separated by Pd−Ag membranes is shown.

According to the results, the minimum separation cost is achieved when the fraction of hydrogen separated by the membrane module is around 70%: when lower fractions are considered, the hydrogen separation cost increases because the EHC needs a higher surface area which significantly increases the cost, whereas the energy consumption decreases for higher relative amount of hydrogen separated by the Pd−Ag membranes. As described previously, the hydrogen separation cost depends on the pressure of the grid. An economic evaluation based on the grid pressure has been performed and the results are shown in Fig. 12. Working at higher grid pressure decreases the hydrogen separation cost due to the smaller membrane surface area required. On the other hand, the purity drops dramatically
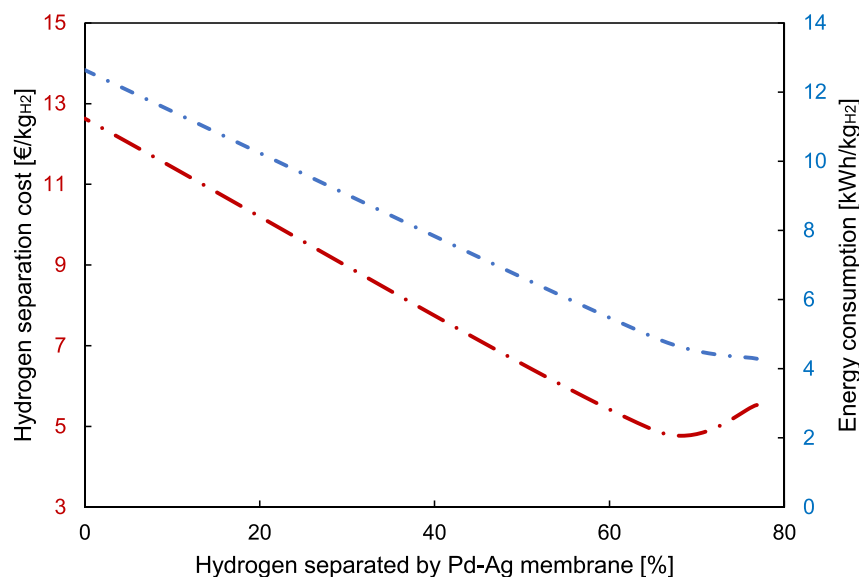
Fig. 11 − Hydrogen separation cost and energy consumption as a function of the hydrogen separated by Pd−Ag membrane.

when working at higher pressure when using the Pd−Ag membranes. Depending on the final users (and the needed purity), it could be interesting to consider the separation from a grid of high pressure.

For the configurations that use sweep gas, the H_2/CH_4 streams have been heated to the working temperature by electricity while the steam has been produced by heat consumption burning natural gas. For a proper comparison between the configurations with sweep gas and the ones with vacuum, a single case in which the steam has been produced also through electricity has been considered.

The energy consumption and the final hydrogen separation costs have been studied. As shown in Fig. 13, producing steam with natural gas is cheaper and the

difference in cost between sweep gas and vacuum configurations increases when electricity is used to produce steam.

In Fig. 14, the pressure at the permeate side of the first membrane module (which is the retentate of the second membrane) in configuration C, has been varied to analyse the effect on the energy consumption and final separation cost. The results show that, when the permeate pressure is reduced, a lower membrane area is required thanks to the increased driving force.

As discussed before when comparing the performance of Pd−Ag or CMS membranes in configuration C, a lower energy consumption and final separation cost were found for the CMSM. For the case of Pd−Ag membranes, a possible re-use of
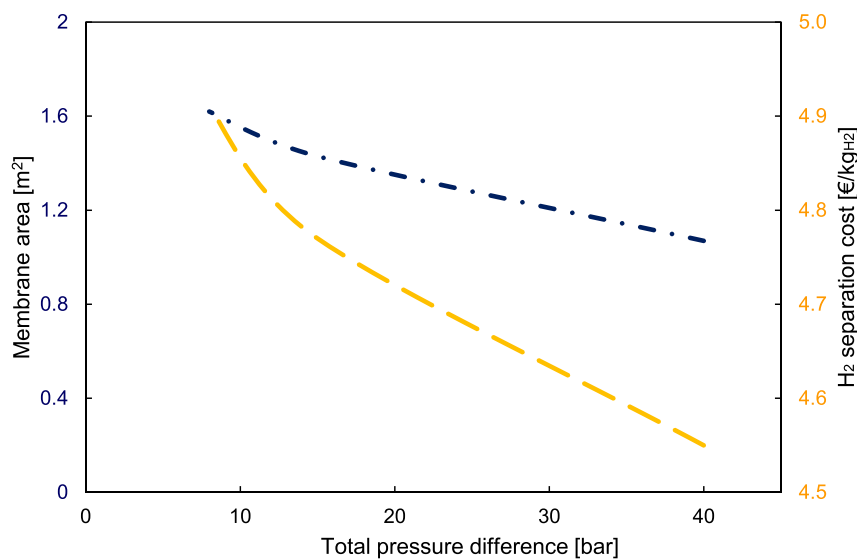

Fig. 12 − Pd−Ag ceramic supported membrane area needed and hydrogen separation cost at different total pressure difference considering configuration A.
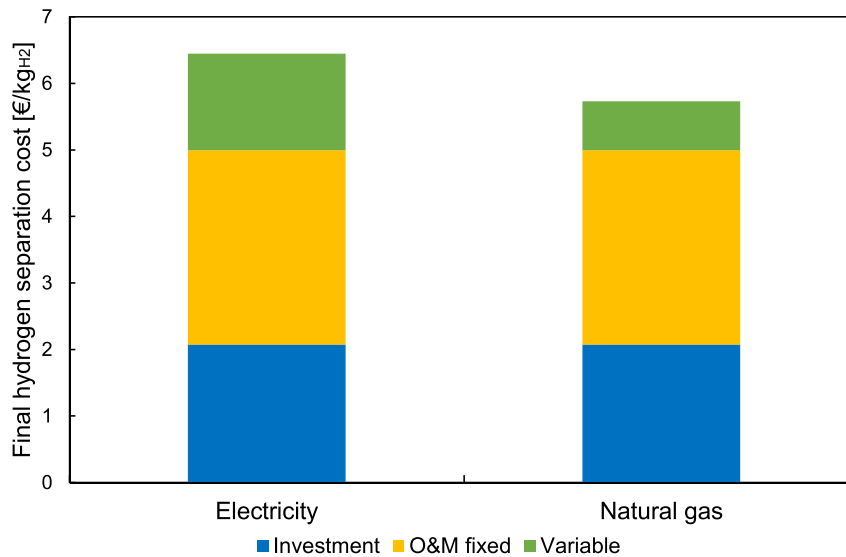
Fig. 13 − **Final hydrogen separation cost distribution in investment, O&M and variable using electricity or natural gas to produce steam as sweep gas in configuration D2.**

the Pd−Ag layer and the support for a cost recovery of 10, 50 and 80% of the membrane cost has been considered to compare the final separation cost with the CMSM. The results are shown in Fig. 15. According to the results, if the membrane layer and support re-use contributes only to 10% of the membrane cost recovery, then it is still more convenient to work with the CMSM in configuration C. On the other hand, above a 50% recovery of the cost, then the use of Pd−Ag membranes is cheaper and more convenient. In configuration C, only the recovery of the membrane layer and support of the Pd−Ag membrane has been considered (which is only the second membrane module).

Configuration D2, which is based on the use of sweep gas to increase the hydrogen partial pressure across the membrane,

has been studied at different sweep gas flow rates to better understand its influence on the heat consumption and final hydrogen separation cost. The results summarized in Fig. 16, show that the heat consumption is proportional to the sweep gas flow rate, while the final separation cost has a minimum at around 1 kmol/h. The main parameters affecting the costs are the heat consumption and the membrane surface area. While the heat consumption increases linearly with the sweep gas flow rate, the membrane area is initially reduced and then remains almost constant with the sweep gas flow rate, to separate the same hydrogen flow rate. According to literature, the sweep gas increases the pressure drop over the porous support, causing a reduction of the hydrogen flow rate separated at higher sweep gas flow rates [8].
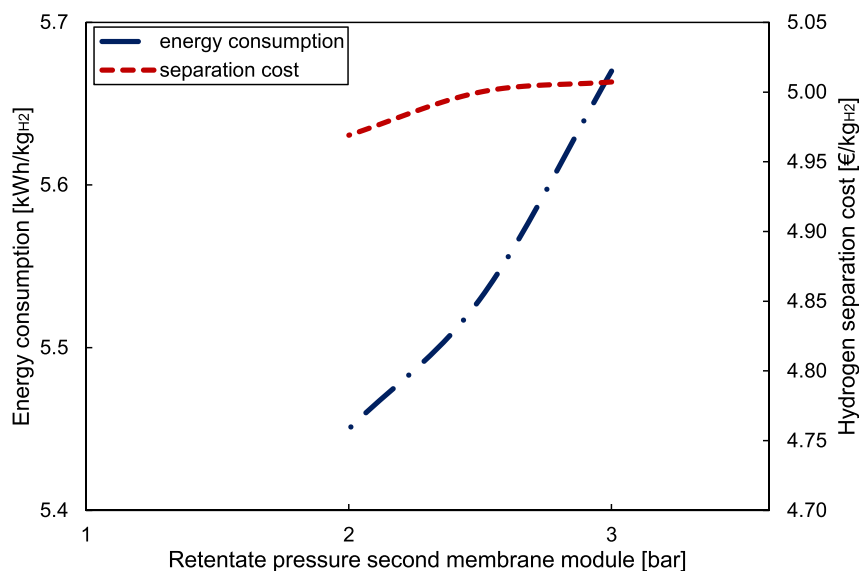

Fig. 14 − **Sensitivity analysis on permeate pressure of first membrane module on configuration C, C4 and C5.**
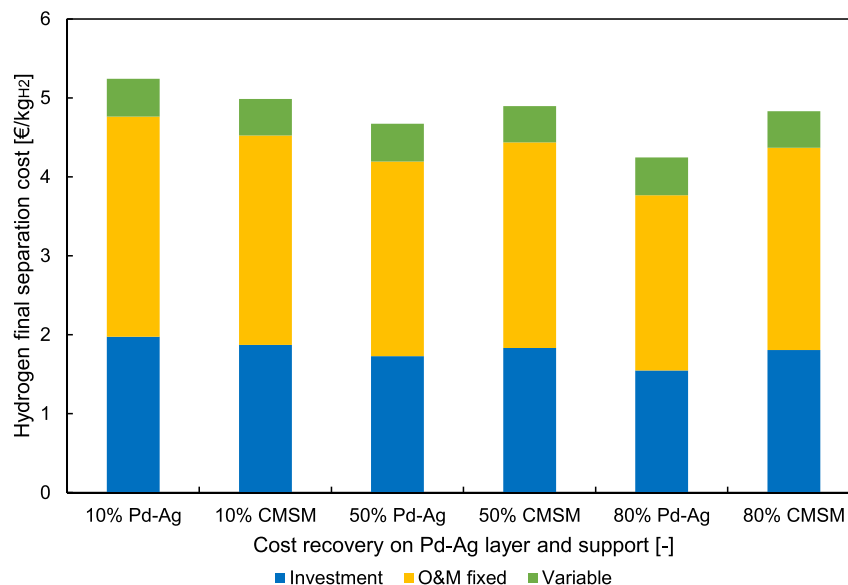
Fig. 15 – Hydrogen separation cost in configuration C and C1, with CMSM and Pd–Ag membrane, considering a recovery of the membrane cost from 10 to 80%.
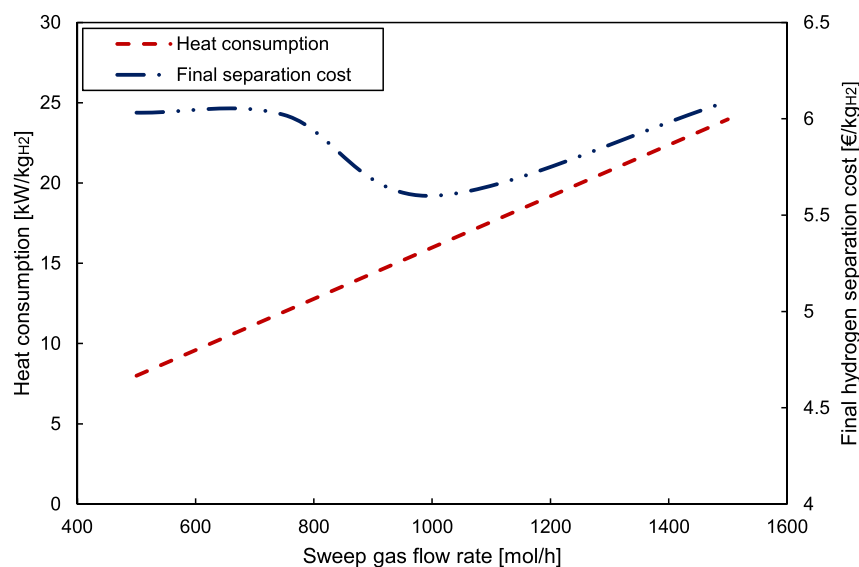

Fig. 16 – Heat consumption and final separation cost trend with a sweep gas flow rate in configuration D2.

Conclusions

Different configurations were proposed for hydrogen separation, mainly based on seven master cases which allow to reach a high hydrogen recovery factor and purity. Two different cases have been considered: a low-pressure grid (up to 8 bar) and a high-pressure grid (from 40 to 80 bar). Moreover, from these main configurations, it is possible to maximize either the recovery or the purity, changing several variables such as the membrane materials, the retentate or permeate pressure and membrane type.

When considering the low-pressure grid, the best master configuration in terms of energy consumption and hydrogen separation cost is C which is based only on a membrane module and a vacuum pump. On the other hand, it does not reach a very high purity (99.92%). To improve the final purity, configuration B provides the optimum solution, which thanks to the two membrane modules, guarantees very high hydrogen purity (99.99%). The main drawback is the energy consumption of 7.95 kWh/kg_{H2}. Depending on the application required by the users, it is worthwhile to select a more energy-consuming configuration which reaches very high purity or saving the consumption at the expense of the purity.

Choosing a metallic membrane support, as in configuration A1 and D2, the hydrogen purity is increased, but the final hydrogen separation cost increases to 11 and 9.80 €/kg_{H2}, respectively. Configurations A3 and A4 go in the direction of higher retentate pressure with Pd–Ag and CMSM respectively, which allow a higher hydrogen driving force resulting in a

larger HRF and a less pure hydrogen stream (especially for configuration A4). Carbon molecular sieve membranes achieve a lower purity than double-skin Pd−Ag membranes, especially at low pressure, on the other hand they have an important advantage over Pd−Ag membranes, which is the lower energy consumption required thanks to the lower operating temperature at which they work. Moreover, they are cheaper, which generally results in a lower hydrogen separation cost.

When considering the configurations to separate H_2 coming from high-pressure natural gas grid, configuration C, based on CMSM, Pd−Ag membrane, vacuum pump and EHC, achieves an extremely high purity (99.99%) at average hydrogen separation cost (5.05 €/kg_{H2}). It is even possible to reduce this cost by decreasing the permeate pressure of the first membrane module, as shown in Table 3 and Fig. 8, for configurations C4 and C5. It is worth mentioning that configuration C1 has the same layout as configuration C, with the only difference in the membrane type chosen. Indeed, configuration C1 used in the first membrane module an ultra-thin Pd−Ag membrane. This configuration shows a higher energy consumption and final separation cost because the CMSM operated at high pressures, are more convenient than the Pd−Ag membrane.

All the considered configurations for hydrogen production of 25 kg/day require an electric consumption in the range of 3.94 and 12.63 kWh/kg_{H2} with a final separation cost (except for the configuration in which only the EHC is used) between 3.56 and 9.80 €/kg_{H2} which is quite competitive in comparison to conventional separation systems, such as a PSA unit (20 kWh/kg_{H2} and 8.3 US\$/kg) which could work efficiently mainly at large scale and high hydrogen concentrations in the inlet stream.

Acknowledgments

Appendix

Configuration D1.

The second master configuration, called D1 is depicted in Figure A1.

Configuration D1 is based on the use of sweep gas, which is fed to the membrane permeate side, to increase the membrane driving force instead of applying vacuum. An energy consumption evaluation to compare sweep gas and vacuum is needed. For this configuration, both the electricity and the natural gas have been considered to produce steam. The equal comparison between vacuum and sweep gas must be found when electricity is considered because in the configuration with vacuum, only electricity is assumed. The steam is heated up in two heat exchangers and a boiler before entering to the membrane permeate side. The stream coming from the grid reaches the working operating temperature in a heat exchanger and a heater before being fed to the membrane module. The module is a double-skin Pd−Ag ceramic supported membrane with a permeance of $2 \cdot 10^{-6}$ mol/s/m²/Pa and a H_2/CH_4 selectivity of 65,000. 1 kmol/h of steam was assumed as sweep gas. The grid and retentate stream are at 8 bar, while the permeate is at 1 bar. The permeate stream is cooled and the water is condensed before the temperature swing adsorption unit, where a further water removal is achieved. After the TSA, which operates at 70 °C, the stream is sent to the EHC where more hydrogen is recovered. Different sweep gas flow rates have been considered for a proper understanding of the effect on hydrogen recovery, purity, electricity consumption and costs. Configuration D2 is based on D1 with the difference of a metallic supported Pd−Ag membrane.
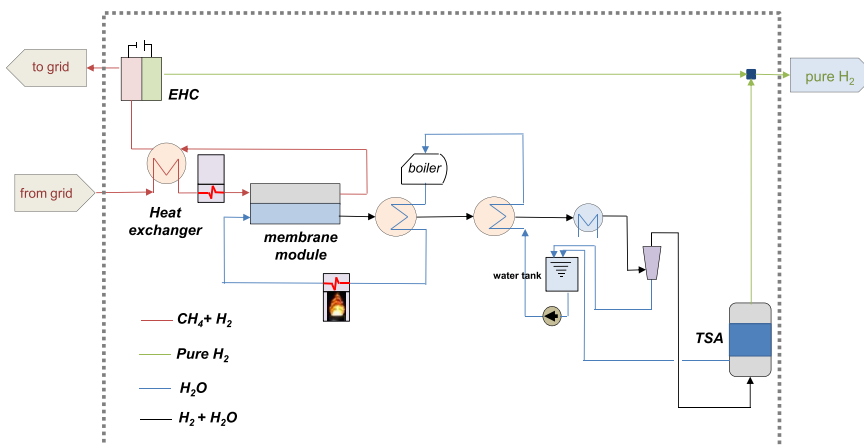
Configuration A5.

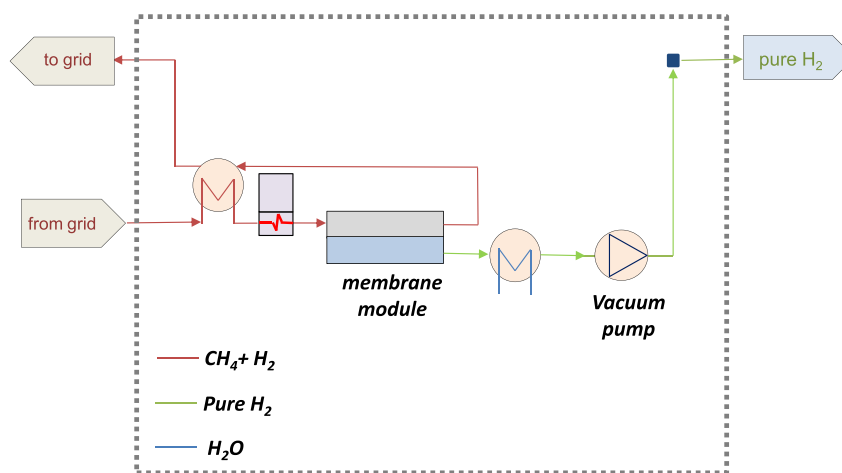Fig. A1 − Process flow diagram of configuration D1.

Fig. A2 — Process flow diagram of configuration A5.2

The following master configuration, A5, is shown in Figure A2. The hybrid system is based only on a membrane module and the vacuum pump without the electrochemical hydrogen compressor component. The membrane module has a hydrogen permeance of 10^{-6} mol/s/m^2/Pa and a H$_2$/CH$_4$

proposed configuration is the membrane module; hence a large surface area is required to achieve the hydrogen rate required.
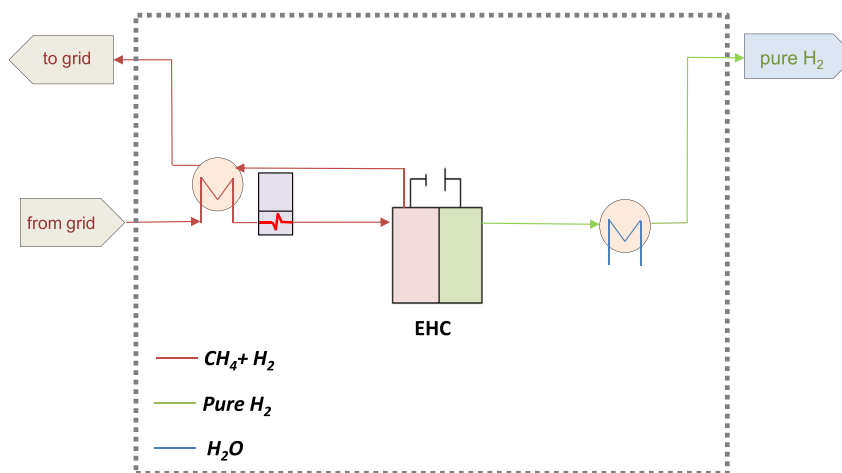
Configuration A6.

Fig. A3 — Process flow diagram of configuration A6.3

selectivity at 1 bar of 200,000 [41]. This configuration has been adopted to evaluate the hydrogen separation cost when the electrochemical hydrogen compressor is not included. The Pd—Ag membrane considered is metallic supported to reach the hydrogen purity target. The retentate pressure is 8 bar, while the vacuum reaches 100 mbar. The inlet stream is electrically heated to 400 °C which is the membrane working temperature. The retentate side of the membrane is sent back to the natural gas grid. The only separation unit in the

This configuration A6 consists only of the electrochemical hydrogen compressor as shown in Figure A3. The working temperature is 65 °C, anode and cathode side at 8 bar. The inlet stream is fed to a heat exchanger and is then electrically heated in a heater before being fed to the EHC. It is interesting to study the energy consumption and hydrogen separation cost associated to the EHC, especially in comparison to the previous proposed configurations.

Abbreviations

CMSM   Carbon molecular sieve membrane
Pd-Ag membrane   Palladium-silver membrane
EHC   Electrochemical hydrogen compressor
PSA   Pressure swing adsorption
TSA   Temperature swing adsorption
CAPEX   Capital expense
OPEX   Operating expense
NG   Natural gas
c-PdDS   Ceramic supported Pd-Ag double skin membrane
c-tPd   Thin ceramic supported Pd-Ag membrane
c-Pd   Ceramic supported Pd-Ag membrane
TOC   Total overnight cost
CCF   Capital charge factor
BEC   Bare Erected cost
HRF   Hydrogen recovery factor

REFERENCES

[1] Harvey R, Abouatallah R, Cargnelli J. PEM electrolysis for hydrogen production: principles and applications. 2016. p. 389.

[2] Melaina M, Penev M, Steward D, Antonia O, Bush B, Daniel B, Heimiller D, Melius J. Hydrogen infrastructure cost estimates and blending hydrogen into natural gas pipelines. 2012.

[3] Knaebel SP, Ko DH, Biegler LT. Simulation and optimization of a pressure swing adsorption system: recovering hydrogen from methane. Adsorpt Int Adsorpt Soc 2005;11:615–20. https://doi.org/10.1007/s10450-005-5994-4.

[4] Grande CA. Advances in pressure swing adsorption for gas separation. ISRN Chem Eng 2012;(2012):1–13. https://doi.org/10.5402/2012/982934.

[5] Melaina MW, Antonia O, Penev M. Blending hydrogen into natural gas pipeline networks. Rev Key Issues 2013. https://doi.org/10.2172/1219920.

[6] Yang J, Lee CH, Chang JW. Separation of hydrogen mixtures by a two-bed pressure swing adsorption process using zeolite 5A. Ind Eng Chem Res 1997;36:2789–98. https://doi.org/10.1021/ie960728h.

[7] Di Marcoberardino G, Vitali D, Spinelli F, Binotti M. Green hydrogen production from raw biogas: a techno-economic investigation of conventional processes using pressure swing adsorption unit. Processes 2018;6:19. https://doi.org/10.3390/pr6030019.

[8] Nordio M, Soresi S, Manzolini G, Melendez J, Van Sint Annaland M, Pacheco Tanaka DA, Gallucci F. Effect of sweep gas on hydrogen permeation of supported Pd membranes: experimental and modeling. Int J Hydrogen Energy 2019;44:4228–39. https://doi.org/10.1016/j.ijhydene.2018.12.137.

[9] Pinacci P, Drago F. Influence of the support on permeation of palladium composite membranes in presence of sweep gas. Catal Today 2012;193:186–93. https://doi.org/10.1016/j.cattod.2012.02.041.

[10] Unal A. Gaseous mass transport in porous media through a stagnant gas. Ind Eng Chem Res 1987;26:72–7. https://doi.org/10.1021/ie00061a013.

[11] Boon J, Pieterse JAZ, Dijkstra JW, van Sint Annaland M. Modelling and systematic experimental investigation of mass transfer in supported palladium-based membrane separators. Int J Greenh Gas Control 2012;11:122–9. https://doi.org/10.1016/j.ijggc.2012.09.014.

[12] Llosa Tanco MA, Pacheco Tanaka DA, Rodrigues SC, Texeira M, Mendes A. Composite-alumina-carbon molecular sieve membranes prepared from novolac resin and boehmite. Part I: preparation, characterization and gas permeation studies. Int J Hydrogen Energy 2015;40:5653–63. https://doi.org/10.1016/j.ijhydene.2015.02.112.

[13] Llosa Tanco MA, Pacheco Tanaka DA, Mendes A. Composite-alumina-carbon molecular sieve membranes prepared from novolac resin and boehmite. Part II: effect of the carbonization temperature on the gas permeation properties. Int J Hydrogen Energy 2015;40:3485–96. https://doi.org/10.1016/j.ijhydene.2014.11.025.

[14] Llosa Tanco MA, Pacheco Tanaka DA, Mendes A. Composite-alumina-carbon molecular sieve membranes prepared from novolac resin and boehmite. Part II: effect of the carbonization temperature on the gas permeation properties. Int J Hydrogen Energy 2014;40:3485–96. https://doi.org/10.1016/j.ijhydene.2014.11.025.

[15] Hägg M, Lie JONA, Lindbråthen A. Carbon molecular sieve membranes a promising alternative for selected industrial applications. Ann N Y Acad Sci 2003;345:329–45.

[16] Nordio M, Barain ME, Raymakers L, Annaland MVS, Mulder M, Gallucci F. Effect of CO2 on the performance of an electrochemical hydrogen compressor. Chem Eng J 2019:123647. https://doi.org/10.1016/j.cej.2019.123647.

[17] Salleh WNW, Ismail AF. Carbon membranes for gas separation processes: recent progress and future perspective. J Membr Sci Res 2015;1:2–15. https://doi.org/10.22079/jmsr.2015.12301.

[18] Hamm J, Ambrosi A, Griebeler J, Marcilio N, Tessaro I, Pollo L. Recent advances in the development of supported carbon membranes for gas separation. Int J Hydrogen Energy 2017;42:24830–45. https://doi.org/10.1016/J.IJHYDENE.2017.08.071.

[19] Salleh WNW, Ismail AF, Matsuura T, Abdullah MS. Precursor selection and process conditions in the preparation of carbon membrane for gas separation: a review. Separ Purif Rev 2011;40:261–311. https://doi.org/10.1080/15422119.2011.555648.

[20] Swaidan R, Ma X, Litwiller E, Pinnau I. High pressure pure- and mixed-gas separation of CO 2/CH 4 by thermally-rearranged and carbon molecular sieve membranes derived from a polyimide of intrinsic microporosity. J Membr Sci 2013;447:387–94. https://doi.org/10.1016/j.memsci.2013.07.057.

[21] Ding L, Wei Y, Li L, Zhang T, Wang H, Xue J, Ding LX, Wang S, Caro J, Gogotsi Y. MXene molecular sieving membranes for highly efficient gas separation. Nat Commun 2018;9:1–7. https://doi.org/10.1038/s41467-017-02529-6.

[22] Jin H, Wollbrink A, Yao R, Li Y, Caro J, Yang W. A novel CAU-10-H MOF membrane for hydrogen separation under hydrothermal conditions. J Membr Sci 2016;513:40–6. https://doi.org/10.1016/j.memsci.2016.04.017.

[23] Nordio M, Rizzi F, Manzolini G, Mulder M, Raymakers L, Van Sint Annaland M, Gallucci F. Experimental and modelling study of an electrochemical hydrogen compressor. Chem Eng J 2019;369:432–42. https://doi.org/10.1016/j.cej.2019.03.106.

[24] De-fg-er DOEG, De-fg-er DOEG, De-fg-er DOEG. Electrochemical hydrogen compressor. 2006.

[25] Clausse M, Merel J, Meunier F. Numerical parametric study on CO2 capture by indirect thermal swing adsorption. Int J Greenh Gas Control 2011;5:1206–13. https://doi.org/10.1016/j.ijggc.2011.05.036.

[26] April M. Cost estimation methodology. 2011.

[27] Ulleberg Ø, Hancke R. Techno-economic calculations of small-scale hydrogen supply systems for zero emission

transport in Norway. Int J Hydrogen Energy 2020;45:1201–11. https://doi.org/10.1016/j.ijhydene.2019.05.170.

[28] Sara HR, Enrico B, Mauro V, Andrea DC, Vincenzo N. Techno-economic analysis of hydrogen production using biomass gasification -a small scale power plant study. Energy Procedia 2016;101:806–13. https://doi.org/10.1016/j.egypro.2016.11.102.

[29] Rubin ES. Understanding the pitfalls of CCS cost estimates. Int J Greenh Gas Control 2012;10:181–90. https://doi.org/10.1016/j.ijggc.2012.06.004.

[30] Spallina V, Velarde IC, Jimenez JAM, Godini HR, Gallucci F, Van Sint Annaland M. Techno-economic assessment of different routes for olefins production through the oxidative coupling of methane (OCM): advances in benchmark technologies. Energy Convers Manag 2017;154:244–61. https://doi.org/10.1016/j.enconman.2017.10.061.

[31] DACE cost and value. DACE Price Bookl 2017;31:190.

[32] Fernandez E. Natural gas membrane reformer for M -CHP applications WP3 – membrane development and scale-up report on development of new membranes for WP4. 2017. https://doi.org/FCH-JU-2013-1.

[33] Caravella A, Barbieri G, Drioli E. Effect of the concentration polarization on the hydrogen permeation through pd-based membranes. Chem Eng Trans 2009;17:1681–6. https://doi.org/10.3303/CET0917281.

[34] Nakajima T, Kume T, Ikeda Y, Shiraki M, Kurokawa H, Iseki T, Kajitani M, Tanaka H, Hikosaka H, Takagi Y, Ito M. Effect of concentration polarization on hydrogen production performance of ceramic-supported Pd membrane module. Int J Hydrogen Energy 2015;40:11451–6. https://doi.org/10.1016/j.ijhydene.2015.03.088.

[35] Peters TA, Stange M, Klette H, Bredesen R. High pressure performance of thin Pd-23%Ag/stainless steel composite membranes in water gas shift gas mixtures; influence of dilution, mass transfer and surface effects on the hydrogen flux. J Membr Sci 2008;316:119–27. https://doi.org/10.1016/j.memsci.2007.08.056.

[36] Peters TA, Tucho WM, Ramachandran A, Stange M, Walmsley JC, Holmestad R, Borg A, Bredesen R. Thin Pd-23% Ag/stainless steel composite membranes: long-term stability, life-time estimation and post-process characterisation. J Membr Sci 2009;326:572–81. https://doi.org/10.1016/j.memsci.2008.10.053.

[37] He X. Techno-economic feasibility analysis on carbon membranes for hydrogen purification. Separ Purif Technol 2017;186:117–24. https://doi.org/10.1016/j.seppur.2017.05.034.

[38] Tosti S, Basile A, Bettinali L, Borgognoni F, Gallucci F, Rizzello C. Design and process study of Pd membrane reactors. Int J Hydrogen Energy 2008;33:5098–105. https://doi.org/10.1016/j.ijhydene.2008.05.031.

[39] Chen H, Pei P, Song M. Lifetime prediction and the economic lifetime of Proton Exchange Membrane fuel cells. Appl Energy 2015;142:154–63. https://doi.org/10.1016/j.apenergy.2014.12.062.

[40] Wendel CH, Braun RJ. Design and techno-economic analysis of high efficiency reversible solid oxide cell systems for distributed energy storage. Appl Energy 2016;172:118–31. https://doi.org/10.1016/j.apenergy.2016.03.054.

[41] J.A. Medrano, E. Fernandez, J. Melendez, M. Parco, D.A. Pacheco, High temperature stability of Pd-alloy metallic supported membranes and tests in a fluidized bed reactor for autothermal steam methane reforming, (n.d.).